International Conference on Automation, Control, Engineering and Computer Science (ACECS'14)
Proceedings - Copyright IPCO-2014, pp.116-122
ISSN 2356-5608

Control of Chaos in an Impact Mechanical Oscillator

Hassène Gritli
Direction Générale des Etudes Technologiques
Institut Supérieur des Etudes Technologiques
de Kélibia
8090 Kélibia, Tunis, Tunisia
Email: grhass@yahoo.fr

Safya Belghith
Université de Tunis El Manar
Ecole Nationale d'Ingénieurs
de Tunis
1002 Tunis, Tunisia
Email: safya.belghith@enit.rnu.tn

Nahla Khraief
Université de Carthage
Ecole Supérieure de Technologie
et d'Informatique
2035 Charguia II, Tunis, Tunisia
Email: nahla_khraief@yahoo.fr

***Abstract*—This paper deals with the control of chaos exhibited by an impacting mechanical oscillator of one-degree-of-freedom. Its mathematical model is represented by an impulsive hybrid non-autonomous linear dynamics. This dynamics can display attractive nonlinear phenomena such as bifurcations and chaos. In this paper, we propose an approach to control chaos. The proposed strategy is based primarily on the OGY method. First, we derive an analytical expression of a constrained controlled Poincaré map where. Its fixed point is identified numerically. Then we determine the linearized controlled Poincaré map around this fixed point. Based on this linearized map, we will design a state feedback controller to stabilize the fixed point and then to control chaos.**

I. Introduction

It is recognized that chaos occurs frequently in many areas of science and engineering and in a wide variety of nonlinear dynamical systems such as nonlinear oscillators [1], [2], impact mechanical systems [3], [4], [11], [18], [10], [26], walking robots [5], [6], [7], [8], etc. Nonlinear dynamics of impact oscillators and their nonlinear behaviors have received considerable theoretical and experimental attentions in the past. Many mathematical-experimental studies of the impact systems have been conducted, and a particular interest has been focused on the analysis and control of chaos and bifurcations [11].More general studies of multiple-degree-of-freedom impact mechanical oscillators were also conducted [12], [13], [14], [18], [10]. However, almost all these studies focus primarily on one single impact. In this paper, we will examine a mechanical oscillator of one-degree-of-freedom with one impact rigid constraint. This mechanical system is periodically excited by an external sinusoidal input. This oscillator consists of a mass, coupled with a spring and a damper, and the mass movement is limited by the single rigid constraint [15], [16], [17], [19], [26]. This envisaged impact system is classified as a non-autonomous impulsive hybrid linear dynamics that can generate chaos and bifurcations.

The design of an efficient approach to control chaos is a central point in the field of nonlinear science. In the literature, many methods and strategies for chaos control in nonlinear dynamical systems have been proposed [20], [21], [22], [23]. It is known so far that there are an infinite number of unstable periodic orbits (UPOs) within a chaotic attractor. Moreover, the trajectory of a system is very often in the vicinity of each of them. Typically, chaos control was used to stabilize a desired UPO for some given set of parameters. In the immense interest to control chaos, Ott *et al.* [24] made the following two ideas [9], [20], [23]: (1) controller design for discrete system model based on the linearization of the Poincaré map, and (2) using the property of recurrence of chaotic trajectories and the application of control action at the moments when the trajectory returns to a neighborhood of the desired state (or orbit). This method is mainly based on the linearization of the Poincaré map and it is known as the OGY method.

In this paper, we will use the OGY method to control chaos exhibited in the impulsive hybrid dynamic linear non-autonomous mechanical oscillator. We will acquire from this hybrid dynamics an explicit expression of a constrained controlled Poincaré map. Based on this constrained map, we will determine an UPO (or a fixed point in the UPO) where its stability will be analyzed using the linearized Poincaré map. Based on this linearized map, we will design a state feedback controller. Relying on the second key of the OGY method, the designed controller will be applied at the beginning of each period.

This paper is structured in eight sections. In Section II, the impulsive hybrid linear dynamics of the impact mechanical oscillator is given. The periodic and chaotic behaviors of the impact oscillator are also discussed briefly in this section. Section III is dedicated for the development of an analytical expression of the constrained controlled Poincaré map. The procedure of determination of fixed points based on the constrained Poincaré map is addressed in Section IV. Section V gives the linearized controlled Poincaré map. The problem of stabilization of an unstable fixed point and so the control of chaos is treated in Section VI. We present in Section VII some numerical simulations showing the control of chaos in the impulsive hybrid dynamics of the impact oscillator. Finally in Section VIII, some conclusions are noted.

II. Impulsive Hybrid Linear Dynamics of the Impact Oscillator

A. Impact Mechanical Oscillator

We consider in this work a non-smooth dynamical system: an oscillating mechanical system with impact known as the impact mechanical oscillator (Figure 1). This impact oscillator consists of a mass m. This mass is connected to the wall through both a spring having a stiffness k and with a damping coefficient c. A second wall introduced as a rigid constraint is deviated from the mass of a distance d. The mass is excited periodically via a sinusoidal input $u(t) = U_m cos(wt)$ where w and U_m are the excitation frequency and the excitation amplitude, respectively . Under this oscillating input and from

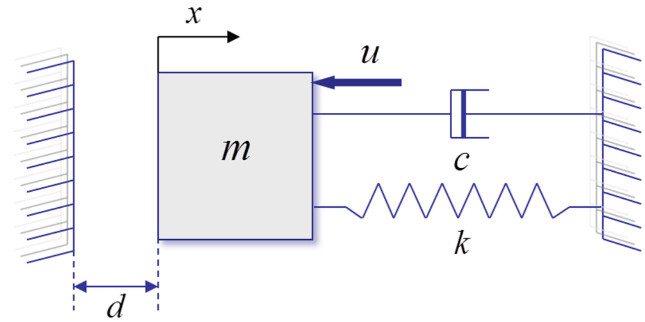

Fig. 1. The impact mechanical oscillator with a single rigid constraint.

an initial state at time $t_0 = 0$s, the mechanical system will oscillate on the horizontal axis x and therefore the mass will produce impacts with the wall on the left for $x = d$. At each impact, the velocity of the mass undergoes a restitution having a coefficient r. However, the position of the mass is not changed and no slippage occurs at impact. Let $T = \frac{2\pi}{w}$ be the period of oscillation and τ is the impact time at which the mass hits the wall.

B. Impulsive Hybrid Non-Autonomous Linear Dynamics

The dynamics of the impact mechanical oscillator is composed of two phases: an oscillation phase and an instantaneous impact phase. Let $\boldsymbol{z} = [\begin{array}{cc} x & \dot{x} \end{array}]^T$ be the state vector where x and $\dot{x}$ are the displacement and the velocity components, respectively. The impulsive hybrid linear non-autonomous dynamics of the impact mechanical oscillator is given by:

$$\dot{\boldsymbol{z}} = \boldsymbol{\mathcal{A}}\boldsymbol{z} + \boldsymbol{\mathcal{B}}u(t), \qquad \text{if} \quad \boldsymbol{z} \notin \Gamma \tag{1}$$

$$\boldsymbol{z}^+ = \boldsymbol{\mathcal{R}}\boldsymbol{z}^-, \qquad \text{if} \quad \boldsymbol{z} \in \Gamma \tag{2}$$

where subscribes $^+$ and $^-$ denotes just after and just before the impact phase, respectively.

In (1) and (2), the different matrices are defined as: $\boldsymbol{\mathcal{A}} = \begin{bmatrix} 0 & 1 \\ -\frac{k}{m} & -\frac{c}{m} \end{bmatrix}$, $\boldsymbol{\mathcal{B}} = \begin{bmatrix} 0 \\ -\frac{1}{m} \end{bmatrix}$ and $\boldsymbol{\mathcal{R}} = \begin{bmatrix} 1 & 0 \\ 0 & -r \end{bmatrix}$.

In fact, linear differential equation (1) describes the non-autonomous linear dynamics during the swing phase. However, the algebraic equation (2) offers the impulsive impact during the impact phase. All these equations form the impulsive hybrid non-autonomous linear dynamics of the impact mechanical oscillator. In (1) and (2), Γ defines the impact condition (surface). It is defined by:

$$\Gamma = \left\{ \boldsymbol{z} \in \Re^{2\times 1},\ h(\boldsymbol{z}) = \boldsymbol{\mathcal{C}}\boldsymbol{z} - d = 0 \right\}, \tag{3}$$

with $\boldsymbol{\mathcal{C}} = [\begin{array}{cc} 1 & 0 \end{array}]$. In fact, while oscillating, the mass m is subject to one unilateral constraint defined by $h(\boldsymbol{z}) > 0$.

C. Periodic and Chaotic Behaviors

The impact mechanical oscillator may generate periodic and chaotic behavior with respect to parameters of bifurcation r, d and w [15], [16], [17], [19]. In this paper, we choose $m = 1\,Kg$, $k = 1\,N/m$, $c = 0\,N/(m/s)$, $d = 0\,m$, $r = 0.8$ and $U_m = -1\,N$. To study the nonlinear dynamics of the impact mechanical oscillator through bifurcation diagrams, it is essential to choose a Poincaré section Λ which includes all intersection points. This Poincaré section Λ should be transverse to the system trajectory (1)-(3). These points are then reported in the bifurcation diagrams as a system parameter changes. Since the dynamics is non-autonomous, the choice of a suitable Poincaré section Λ is:

$$\Lambda = \{t \geq 0, s(t) = t - (n-1)\,T = 0,\ n = 1, 2, \ldots\}. \tag{4}$$

Figure 2 gives the bifurcation diagram with respect to the excitation frequency w. This bifurcation diagram shows the speed of the mass on the Poincaré section (4). Figure 3 gives a hybrid limit cycle showing a periodic oscillation of period 1. This limit cycle shows that the mechanical oscillator undergoes a single impact in one period T. However, the chaotic attractor in Figure 4 shows that the impact oscillator can undergo several impacts during a single period T. In this work, we will not consider the case of multiple impacts. We will interest only in the case where there is only one impact during the period T.

Therefore, our main objective is to control chaos in the impulsive hybrid linear dynamics of the impact mechanical oscillator. Then, our goal is to transform the chaotic behavior of the oscillator into a period-1 oscillation. This is will be done by stabilizing it based on some control approach. Thus, our strategy to control chaos will be processed according to the OGY method in two steps:

1) The first step deals with the numerical identification of an unstable limit cycle (or an unstable periodic orbit) within a chaotic attractor for some bifurcation parameter w. This will be done by the design of an explicit expression of a controlled Poincaré map.
2) The second step lies in the stabilization of this unstable limit cycle by designing a specific controller based on the linearization of the controlled Poincaré map.

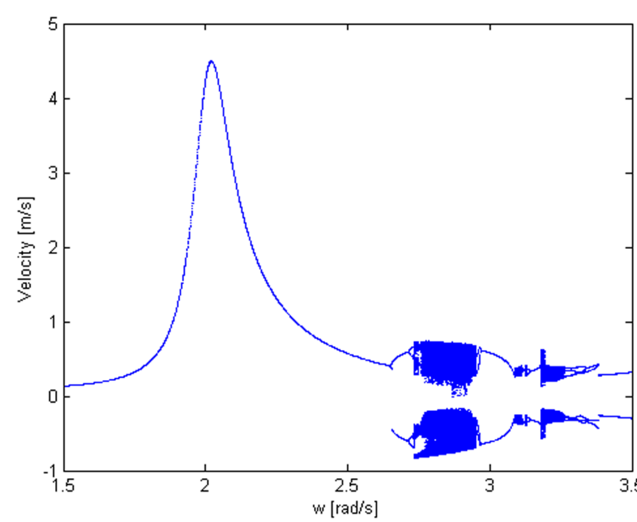

Fig. 2. Bifurcation diagram: velocity of the mass as a function of the excitation frequency w.

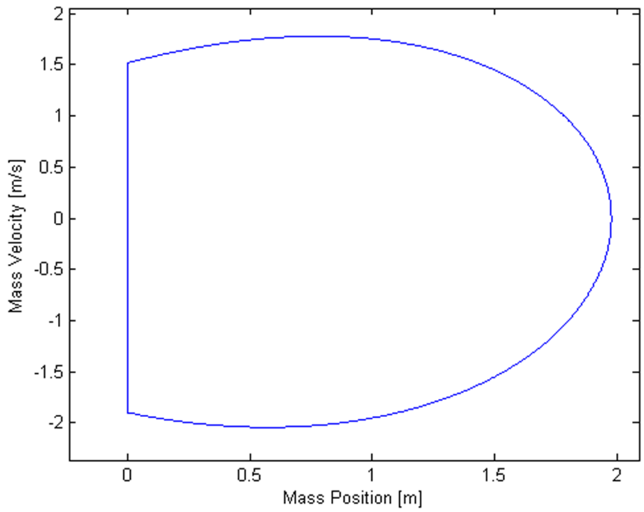

Fig. 3. A 1-period nominal limit cycle of the impact oscillator for $w = 2.2\,rad/s$.

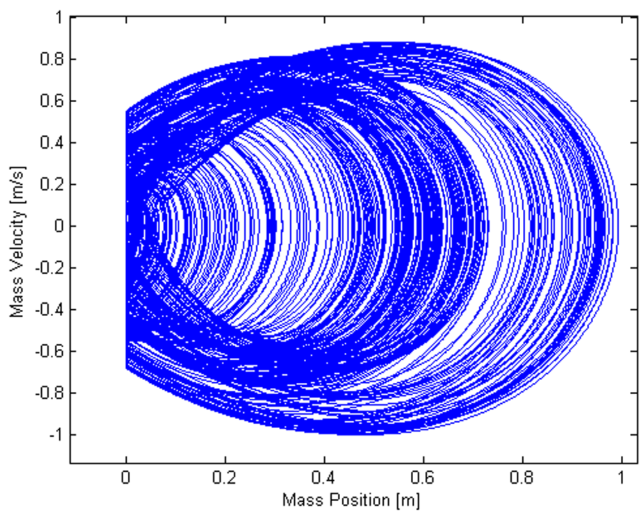

Fig. 4. A chaotic attractor of the impact oscillator for $w = 2.8\,rad/s$.

III. Determination of the Controlled Poincare Map

A controlled Poincaré map is the one with a controller v which will be designed. Then, to control chaos displayed in the impulsive hybrid linear dynamics (1)-(3), we will add the controller v to the excitation input u. Thus, following our control strategy, the proposed controller v must be constant during the n^{th} period T, i.e. $v(t) = v_n$ for all $(n-1)T \leq t \leq nT$, with $n = 1, 2, \ldots$. Thus, the impulsive hybrid dynamics (1)-(2) of the impact mechanical oscillator becomes:

$$\dot{\boldsymbol{z}} = \boldsymbol{\mathcal{A}}\boldsymbol{z} + \boldsymbol{\mathcal{B}}u(t) + \boldsymbol{\mathcal{B}}v_n, \qquad \text{if} \quad \boldsymbol{z} \notin \Gamma \tag{5}$$

$$\boldsymbol{z}^+ = \boldsymbol{\mathcal{R}}\boldsymbol{z}^-, \qquad \text{if} \quad \boldsymbol{z} \in \Gamma \tag{6}$$

To determine the analytical expression of the controlled Poincaré map, we will consider the Poincare section Λ defined by (4). From an initial condition $\boldsymbol{z}_1 = \boldsymbol{z}(t_0 = 0)$, the mass oscillates before the contact with the impact surface Γ defined by (3). Here, we assume that the initial condition $\boldsymbol{z}_1$ does not belong to Γ. We note τ_1 the time of impact and $\boldsymbol{z}_1^-$ is the state vector just before the impact. Accordingly, the state $\boldsymbol{z}_1^-$ will be passed to the state just after impact $\boldsymbol{z}_1^+$ following (6). Thus, from this state, the mass will oscillate again until the condition $\boldsymbol{z}_2 = \boldsymbol{z}(T)$ defined at the instant T. As a result, we obtain a first cycle that begins with $\boldsymbol{z}_1$ at $0s$ and ends at T with $\boldsymbol{z}_2$. During this cycle, the controller v will remain constant. Then we willl have a first controller v_1 for the first cycle. The state $\boldsymbol{z}_2$ will be used as initial condition for the next cycle, and the mass m oscillates, and so on. Next in this paper, we use the following notations for all $n = 1, 2, \ldots$:

- $\boldsymbol{z}_n$ is the initial condition for the n^{th} cycle,
- τ_n is the impact time for the n^{th} cycle,
- $\boldsymbol{z}_n^-$ is the state just before impact for the n^{th} cycle,
- $\boldsymbol{z}_n^+$ is the state just after impact for the n^{th} cycle,
- v_n is the controller applied during the n^{th} cycle, it is constant between $(n-1)T$ and nT,

Hence, from the condition $\boldsymbol{z}_n$ and get to the next state $\boldsymbol{z}_{n+1}$, the system trajectory goes through three phases: 1^{st} phase of oscillation $\Rightarrow$ 2^{nd} phase of impact $\Rightarrow$ 3^{rd} phase of oscillation. Because the dynamics during the swing phase is governed by the linear non-autonomous system (5) with a sinusoidal input u and a constant controller v, it is easy to determine an explicit expression of a controlled Poincaré map. This Poincaré map relates the states $\boldsymbol{z}_n$ at the beginning of each cycle. Then, to determine the expression of the Poincaré map, we should determine expressions linking the states at the beginning of each phase to those at the end of this phase. The solution of the linear differential equations in (5) is defined by:

$$\boldsymbol{z}(t) = e^{\boldsymbol{\mathcal{A}}(t-t_0)}\boldsymbol{z}(t_0) + e^{\boldsymbol{\mathcal{A}}t}\int_{t_0}^{t} e^{-\boldsymbol{\mathcal{A}}\xi}\mathcal{B}\left(u(\xi) + v\right)d\xi. \tag{7}$$

As $u(t) = U_m cos(wt)$, the state vector $\boldsymbol{z}(t)$ is defined by the following expression:

$$\begin{aligned} \boldsymbol{z}(t) &= e^{\boldsymbol{\mathcal{A}}(t-t_0)}\boldsymbol{z}(t_0) \\ &+\boldsymbol{\mathcal{M}}\left[w\boldsymbol{\mathcal{A}}^{-1}\boldsymbol{\mathcal{B}}sin(wt) - \boldsymbol{\mathcal{B}}cos(wt)\right. \\ &\left.+\, e^{\boldsymbol{\mathcal{A}}(t-t_0)}\left(\boldsymbol{\mathcal{B}}cos(wt_0) - w\boldsymbol{\mathcal{A}}^{-1}\boldsymbol{\mathcal{B}}sin(wt_0)\right)\right] \\ &+\left(e^{\boldsymbol{\mathcal{A}}(t-t_0)} - \boldsymbol{I}_2\right)\boldsymbol{\mathcal{A}}^{-1}\boldsymbol{\mathcal{B}}v \end{aligned} \tag{8}$$

with $\boldsymbol{\mathcal{M}} = U_m\left(\boldsymbol{\mathcal{A}} + w^2\boldsymbol{\mathcal{A}}^{-1}\right)^{-1}$, and $\boldsymbol{I}_2$ is the square identity matrix.

1st phase: oscillation phase: In this first phase, we have $\boldsymbol{z}_n = \boldsymbol{z}((n-1)T)$. At the instant $(n-1)T + \tau_n$, the trajectory undergoes an impact with the state $\boldsymbol{z}_n^- = \boldsymbol{z}((n-1)T + \tau_n)$. Hence, according to (8), we obtain the following expression:

$$\boldsymbol{z}_n^- = \boldsymbol{\mathcal{G}}_1(\tau_n)\boldsymbol{z}_n + \boldsymbol{\mathcal{H}}_1(\tau_n) + \boldsymbol{\mathcal{J}}_1(\tau_n)v_n, \tag{9}$$

with $\boldsymbol{\mathcal{G}}_1(\tau_n) = e^{\boldsymbol{\mathcal{A}}\tau_n}$, $\boldsymbol{\mathcal{J}}_1(\tau_n) = \left(e^{\boldsymbol{\mathcal{A}}\tau_n} - \boldsymbol{I}_2\right)\boldsymbol{\mathcal{A}}^{-1}\boldsymbol{\mathcal{B}}$, and $\boldsymbol{\mathcal{H}}_1(\tau_n) = \boldsymbol{\mathcal{M}}\left(w\boldsymbol{\mathcal{A}}^{-1}\boldsymbol{\mathcal{B}}sin(w\tau_n) - \boldsymbol{\mathcal{B}}cos(w\tau_n) + e^{\boldsymbol{\mathcal{A}}\tau_n}\boldsymbol{\mathcal{B}}\right)$.

Relying on the impact condition (3), we emphasize that $h(\boldsymbol{z}_n^-) = \boldsymbol{\mathcal{C}}\boldsymbol{z}_n^- - d = 0$. Thus, in order that an impact occurs, the initial state $\boldsymbol{z}_n$, the impact time τ_n and the controller v_n must satisfy the following condition:

$$\Psi\left(\boldsymbol{z}_n, \tau_n, v_n\right)=\boldsymbol{\mathcal{G}}_0\left(\tau_n\right) \boldsymbol{z}_n+\boldsymbol{\mathcal{H}}_0\left(\tau_n\right)+\boldsymbol{\mathcal{J}}_0\left(\tau_n\right) v_n=0, \tag{10}$$

with $\boldsymbol{\mathcal{G}}_0\left(\tau_n\right)=\boldsymbol{\mathcal{C}} \boldsymbol{\mathcal{G}}_1\left(\tau_n\right)$, $\boldsymbol{\mathcal{H}}_0\left(\tau_n\right)=\boldsymbol{\mathcal{C}} \boldsymbol{\mathcal{H}}_1\left(\tau_n\right)-d$, and $\boldsymbol{\mathcal{J}}_0\left(\tau_n\right)=\boldsymbol{\mathcal{C}} \boldsymbol{\mathcal{J}}_1\left(\tau_n\right)$.

2nd phase: impact phase: In this instantaneous phase, and based on algebraic equations (6), the state vector just before impact $\boldsymbol{z}_n^-$ is related to state vector of just after impact $\boldsymbol{z}_n^+$ according to the following expression:

$$\boldsymbol{z}_n^+=\boldsymbol{\mathcal{R}} \boldsymbol{z}_n^- . \tag{11}$$

3rd phase: oscillation phase: From the state $\boldsymbol{z}_n^+$, the trajectory evolves according to the expression (8). This third phase ends at time $t=nT$. Thus, we obtain the state vector $\boldsymbol{z}_{n+1}$ as:

$$\boldsymbol{z}_{n+1}=\boldsymbol{\mathcal{G}}_2\left(\tau_n\right) \boldsymbol{z}_n^+ +\boldsymbol{\mathcal{H}}_2\left(\tau_n\right)+\boldsymbol{\mathcal{J}}_2\left(\tau_n\right) v_n, \tag{12}$$

with $\boldsymbol{\mathcal{G}}_2\left(\tau_n\right)=e^{\boldsymbol{\mathcal{A}}\left(T-\tau_n\right)}$, $\boldsymbol{\mathcal{J}}_2\left(\tau_n\right)=\left(\boldsymbol{\mathcal{G}}_2\left(\tau_n\right)-\boldsymbol{I}_2\right) \boldsymbol{\mathcal{A}}^{-1} \boldsymbol{\mathcal{B}}$, and
$\boldsymbol{\mathcal{H}}_2\left(\tau_n\right)=\left(e^{\boldsymbol{\mathcal{A}} T}-\boldsymbol{I}_2\right) \boldsymbol{\mathcal{M}} \boldsymbol{\mathcal{B}}-\boldsymbol{\mathcal{G}}_2\left(\tau_n\right) \boldsymbol{\mathcal{H}}_1\left(\tau_n\right)$.

Using expressions (9)-(12), the constrained controlled Poincaré map is expressed as:

$$\left\{\begin{aligned} \boldsymbol{z}_{n+1} & =\boldsymbol{\mathcal{P}}\left(\boldsymbol{z}_n, \tau_n, v_n\right) \\ 0 & =\Psi\left(\boldsymbol{z}_n, \tau_n, v_n\right) \end{aligned}\right. , \tag{13}$$

with $\boldsymbol{\mathcal{P}}\left(\boldsymbol{z}_n, \tau_n, v_n\right)=\boldsymbol{\mathcal{G}}\left(\tau_n\right) \boldsymbol{z}_n+\boldsymbol{\mathcal{H}}\left(\tau_n\right)+\boldsymbol{\mathcal{J}}\left(\tau_n\right) v_n$, where $\boldsymbol{\mathcal{G}}\left(\tau_n\right)=\boldsymbol{\mathcal{G}}_2\left(\tau_n\right) \boldsymbol{\mathcal{R}} \boldsymbol{\mathcal{G}}_1\left(\tau_n\right)$, $\boldsymbol{\mathcal{H}}\left(\tau_n\right)=\boldsymbol{\mathcal{G}}_2\left(\tau_n\right) \boldsymbol{\mathcal{R}} \boldsymbol{\mathcal{H}}_1\left(\tau_n\right)+\boldsymbol{\mathcal{H}}_2\left(\tau_n\right)$,
$\boldsymbol{\mathcal{J}}\left(\tau_n\right)=\boldsymbol{\mathcal{G}}_2\left(\tau_n\right) \boldsymbol{\mathcal{R}} \boldsymbol{\mathcal{J}}_1\left(\tau_n\right)+\boldsymbol{\mathcal{J}}_2\left(\tau_n\right)$, and the matrix $\Psi\left(\boldsymbol{z}_n, \tau_n, v_n\right)$ is defined in (10).

IV. Identification of an Unstable Periodic Orbit

Identification of an unstable periodic orbit (UPO) within a chaotic attractor for some defined bifurcation parameters lies in the identification of a fixed point of the constrained uncontrolled Poincaré map (13), this means for $v_n=0$, for all $n=1,2,\ldots$. Let $\boldsymbol{z}_*$ be the fixed point of the constrained uncontrolled Poincaré map. Then, the fixed must verify $\boldsymbol{z}_{n+1}=\boldsymbol{z}_n=\boldsymbol{z}_*$. For the fixed point $\boldsymbol{z}_*$, there is an impact time τ_*. Accordingly, for $v_*=0$ and on the basis of (13), the fixed point $\boldsymbol{z}_*$ must satisfy the following expressions:

$$\boldsymbol{\mathcal{P}}\left(\boldsymbol{z}_*, \tau_*\right)-\boldsymbol{z}_*=0, \tag{14}$$

$$\Psi\left(\boldsymbol{z}_*, \tau_*\right)=0 . \tag{15}$$

Based on expressions of $\boldsymbol{\mathcal{P}}\left(\boldsymbol{z}_*, \tau_*\right)$ and $\Psi\left(\boldsymbol{z}_*, \tau_*\right)$, we can show that the impact time τ_* must satisfy:

$$\boldsymbol{\mathcal{G}}_0\left(\tau_*\right)\left(\boldsymbol{I}_2-\boldsymbol{\mathcal{G}}\left(\tau_*\right)\right)^{-1} \boldsymbol{\mathcal{H}}\left(\tau_*\right)+\boldsymbol{\mathcal{H}}_0\left(\tau_*\right)=0, \tag{16}$$

and the fixed point $\boldsymbol{z}_*$ is described by the following expression:

$$\boldsymbol{z}_*=\left(\boldsymbol{I}_2-\boldsymbol{\mathcal{G}}\left(\tau_*\right)\right)^{-1} \boldsymbol{\mathcal{H}}\left(\tau_*\right) . \tag{17}$$

Actually τ_* must be calculated numerically from (16) using the well-known iterative Newton-Raphson scheme [25]. Once the time of impact τ_* is calculated, the fixed point $\boldsymbol{z}_*$ will be then computed according to expression (17).

Now we will analyze stability of the fixed point $\boldsymbol{z}_*$. Then, in order to achieve this task, we must determine the linearized controlled Poincaré map around this fixed point.

V. Determination of the Linearized Controlled Poincare Map

Let noting: $\Delta \boldsymbol{z}_{n+1}=\boldsymbol{z}_{n+1}-\boldsymbol{z}_*$, $\Delta \boldsymbol{z}_n=\boldsymbol{z}_n-\boldsymbol{z}_*$, $\Delta v_n=v_n-v_*$, with $v_*=0$. Using the constrained controlled Poincaré map (13) and relying on expression (14), the linearized controlled Poincaré map is defined by:

$$\Delta \boldsymbol{z}_{n+1}=\mathcal{D} \boldsymbol{\mathcal{P}}_{\boldsymbol{z}_n}\left(\boldsymbol{z}_*, \tau_*, v_*\right) \Delta \boldsymbol{z}_n+\mathcal{D} \boldsymbol{\mathcal{P}}_{v_n}\left(\boldsymbol{z}_*, \tau_*, v_*\right) \Delta v_n , \tag{18}$$

with $\mathcal{D} \boldsymbol{\mathcal{P}}_{\boldsymbol{z}_n}$ is the Jacobean matrix of the Poincaré map with respect to $\boldsymbol{z}_n$, and $\mathcal{D} \boldsymbol{\mathcal{P}}_{v_n}$ is the derivative of the Poincaré map with respect to the controller v_n. These two matrices are evaluated at the fixed point $\boldsymbol{z}_*$ and at the impact time τ_* and for $v_*=0$. They are defined as:

$$\left\{\begin{aligned} \mathcal{D} \boldsymbol{\mathcal{P}}_{\boldsymbol{z}_n}\left(\boldsymbol{z}_n, \tau_n, v_n\right) & =\frac{\partial \boldsymbol{\mathcal{P}}\left(\boldsymbol{z}_n, \tau_n, v_n\right)}{\partial \boldsymbol{z}_n}+\frac{\partial \boldsymbol{\mathcal{P}}\left(\boldsymbol{z}_n, \tau_n, v_n\right)}{\partial \tau_n} \frac{\partial \tau_n}{\partial \boldsymbol{z}_n} \\ \mathcal{D} \boldsymbol{\mathcal{P}}_{v_n}\left(\boldsymbol{z}_n, \tau_n, v_n\right) & =\frac{\partial \boldsymbol{\mathcal{P}}\left(\boldsymbol{z}_n, \tau_n, v_n\right)}{\partial v_n}+\frac{\partial \boldsymbol{\mathcal{P}}\left(\boldsymbol{z}_n, \tau_n, v_n\right)}{\partial \tau_n} \frac{\partial \tau_n}{\partial v_n} \end{aligned}\right. \tag{19}$$

By linearizing the second expression in (13) and based on expression (15), we obtain:

$$\left\{\begin{aligned} \Psi_{\boldsymbol{z}_n}+\Psi_{\tau_n} \frac{\partial \tau_n}{\partial \boldsymbol{z}_n} & =0 \\ \Psi_{v_n}+\Psi_{\tau_n} \frac{\partial \tau_n}{\partial v_n} & =0 \end{aligned}\right. , \tag{20}$$

with $\Psi_{\boldsymbol{z}_n}=\frac{\partial \Psi\left(\boldsymbol{z}_n, \tau_n, v_n\right)}{\partial \boldsymbol{z}_n}$, $\Psi_{\tau_n}=\frac{\partial \Psi\left(\boldsymbol{z}_n, \tau_n, v_n\right)}{\partial \tau_n}$, and $\Psi_{v_n}=\frac{\partial \Psi\left(\boldsymbol{z}_n, \tau_n, v_n\right)}{\partial v_n}$.

Assuming that the quantity Ψ_{τ_n} is nonzero, then using (20), it follows that:

$$\left\{\begin{aligned} \frac{\partial \tau_n}{\partial \boldsymbol{z}_n} & =-\frac{\Psi_{\boldsymbol{z}_n}}{\Psi_{\tau_n}} \\ \frac{\partial \tau_n}{\partial v_n} & =-\frac{\Psi_{v_n}}{\Psi_{\tau_n}} \end{aligned}\right. \tag{21}$$

Substitution of these two expressions (21) into (19) yields to:

$$\left\{\begin{aligned} \mathcal{D} \boldsymbol{\mathcal{P}}_{\boldsymbol{z}_n}\left(\boldsymbol{z}_n, \tau_n, v_n\right) & =\frac{\partial \boldsymbol{\mathcal{P}}\left(\boldsymbol{z}_n, \tau_n, v_n\right)}{\partial \boldsymbol{z}_n}-\frac{\partial \boldsymbol{\mathcal{P}}\left(\boldsymbol{z}_n, \tau_n, v_n\right)}{\partial \tau_n} \frac{\Psi_{\boldsymbol{z}_n}}{\Psi_{\tau_n}} \\ \mathcal{D} \boldsymbol{\mathcal{P}}_{v_n}\left(\boldsymbol{z}_n, \tau_n, v_n\right) & =\frac{\partial \boldsymbol{\mathcal{P}}\left(\boldsymbol{z}_n, \tau_n, v_n\right)}{\partial v_n}-\frac{\partial \boldsymbol{\mathcal{P}}\left(\boldsymbol{z}_n, \tau_n, v_n\right)}{\partial \tau_n} \frac{\Psi_{v_n}}{\Psi_{\tau_n}} \end{aligned}\right. . \tag{22}$$

Stability of the fixed point $\boldsymbol{z}_*$ will be done by analyzing the eigenvalues of the Jacobin matrix $\mathcal{D} \boldsymbol{\mathcal{P}}_{\boldsymbol{z}_n}\left(\boldsymbol{z}_*, \tau_*, v_*\right)$. In fact, this Jacobin matrix admits two eigenvalues. Depending on the position of the two eigenvalues with respect to the unit circle, we can study the stability of the fixed point $\boldsymbol{z}_*$. Sufficient condition for stability is that both eigenvalues are inside the unit circle.

It is noted that for a chaotic attractor or chaotic behavior of the impact mechanical oscillator, its impulsive hybrid dynamics exhibits period-1 unstable limit cycles. Then, after the detection of an unstable fixed point of the unstable limit cycle within the chaotic attractor; our objective is to control chaos by stabilizing the unstable fixed point.

VI. Stabilization of the Fixed Point

Stabilization of a fixed point $\boldsymbol{z}_*$ which was previously determined allows to have a period-1 unstable limit cycle for the impact mechanical oscillator. Thus, we seek to determine the appropriate controller $\Delta v_n = v_n - v_*$, with $v_* = 0$ to stabilize the linearized Poincaré map (18). Then we will adopt a state feedback controller as follows:

$$\Delta v_n = \boldsymbol{\mathcal{K}} \Delta \boldsymbol{z}_n \,, \tag{23}$$

where $\boldsymbol{\mathcal{K}}$ is the matrix gain of the controller v_n.

By defining a Lyapunov function:

$$V\left(\Delta \boldsymbol{z}_n\right) = \Delta \boldsymbol{z}_n{}^T \boldsymbol{\mathcal{S}} \Delta \boldsymbol{z}_n, \tag{24}$$

with $\boldsymbol{\mathcal{S}} = \boldsymbol{\mathcal{S}}^T > 0$, then the linearized controlled Poincaré map (18) is asymptotically stable if the following Linear Matrix Inequality (LMI) is satisfied:

$$\begin{bmatrix} \boldsymbol{\mathcal{S}} & \mathcal{D}\boldsymbol{\mathcal{P}}^*_{\boldsymbol{z}_n} + \mathcal{D}\boldsymbol{\mathcal{P}}^*_{v_n} \boldsymbol{\mathcal{Q}} \\ \left(\mathcal{D}\boldsymbol{\mathcal{P}}^*_{\boldsymbol{z}_n} + \mathcal{D}\boldsymbol{\mathcal{P}}^*_{v_n} \boldsymbol{\mathcal{Q}}\right)^T & \boldsymbol{\mathcal{S}} \end{bmatrix} > 0 \,, \tag{25}$$

with $\mathcal{D}\boldsymbol{\mathcal{P}}^*_{\boldsymbol{z}_n} = \mathcal{D}\boldsymbol{\mathcal{P}}_{\boldsymbol{z}_n}(\boldsymbol{z}_*, \tau_*, v_*)$, $\mathcal{D}\boldsymbol{\mathcal{P}}^*_{v_n} = \mathcal{D}\boldsymbol{\mathcal{P}}_{v_n}(\boldsymbol{z}_*, \tau_*, v_*)$, and $\boldsymbol{\mathcal{Q}} = \boldsymbol{\mathcal{K}}\boldsymbol{\mathcal{S}}$.

The gain $\boldsymbol{\mathcal{K}}$ of the state feedback controller (23) is then defined by

$$\boldsymbol{\mathcal{K}} = \boldsymbol{\mathcal{Q}}\boldsymbol{\mathcal{S}}^{-1}. \tag{26}$$

Therefore, by applying the control law

$$v_n = \boldsymbol{\mathcal{K}}\left(\boldsymbol{z}_n - \boldsymbol{z}_*\right) \,, \tag{27}$$

in the impulsive hybrid linear dynamics (5)-(6), the fixed point $\boldsymbol{z}_*$ and hence the corresponding unstable limit cycle will be stabilized. Accordingly, the erratic chaotic behavior of the impact mechanical oscillator will be controlled.

VII. Effectiveness of the Developed Controller: Numerical Simulations

In this section, we propose to apply the controller v_n to verify its effectiveness in controlling chaos exhibited in the impulsive hybrid dynamics of the impacting mechanical oscillator. Then, relying on Section IV, we have identified the following fixed point $\boldsymbol{z}_* = [\ 0.0083 \quad 0.2982\ ]^T$ of some unstable limit cycle within the chaotic attractor of Figure 4. The corresponding impact time is $\tau_* = 2.2146$s. The eigenvalues of the Jacobian matrix of the constrained Poincaré map are found to be -0.2043 and -3.7295. Because one of these two eigenvalues is outside the unit circle, the identified fixed point (the UPO) is unstable. Stabilization occurs through the controller state feedback (27). Using the LMI in (25), the gain $\boldsymbol{\mathcal{K}}$ of the controller v_n is calculated to be: $\boldsymbol{\mathcal{K}} = [\ 0.4121 \quad -0.4291\ ]$.

Using the impulsive hybrid linear non-autonomous dynamics (5)-(6) with the controller (27), Figure 5 shows the controlled period-1 hybrid limit cycle. In this figure, the solid circle is the fixed point $\boldsymbol{z}_*$ of the unstable limit cycle. Obviously, the fixed point of limit cycle is located very near (in the neighborhood) of the impact surface. Figure 6 shows the temporal evolution of the state vector of the mass. In this figure, solid circles reveal the states of the mass at the beginning of each period T. This plot shows that the chaotic behavior of the impact mechanical oscillator will be transformed to a period-1 trajectory just after 12 seconds. This figure is plotted for an initial condition different to the unstable fixed point. In Figure 7, the time variation of the control law v_n is displayed. It is obvious that when the chaotic behavior of the impact mechanical oscillator is controlled, the value of the controller becomes very low and remains constant around $8.10^{-4}N$. In addition, the maximum value of v_n is approximately about $0.5N$.

VIII. Conclusions

In this paper, we proposed an approach to control chaos exhibited in the impulsive hybrid linear dynamics of an impact mechanical oscillator. Our control strategy is chiefly based on the OGY method, which is based on the linearized Poincaré map. Thus, we have constructed an explicit expression of a constrained controlled Poincaré map. Based on this map, we identified its fixed point. In addition, we determined the linearized controlled Poincaré map. Based on this linearized

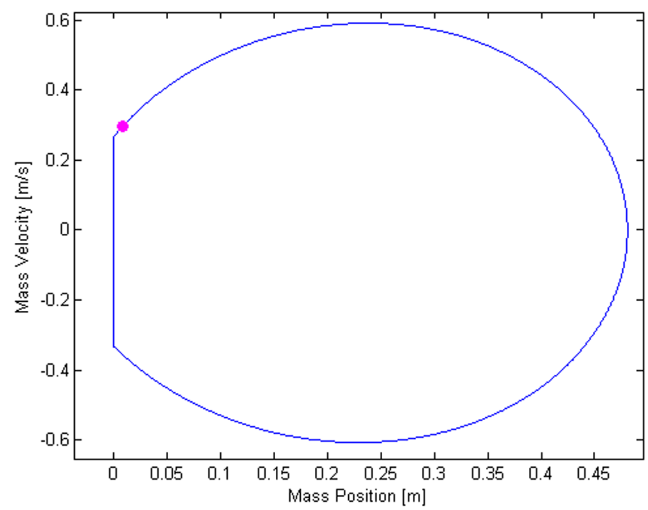

Fig. 5. Controlled limit cycle of the impact oscillator for $w = 2.8\,rad/s$.

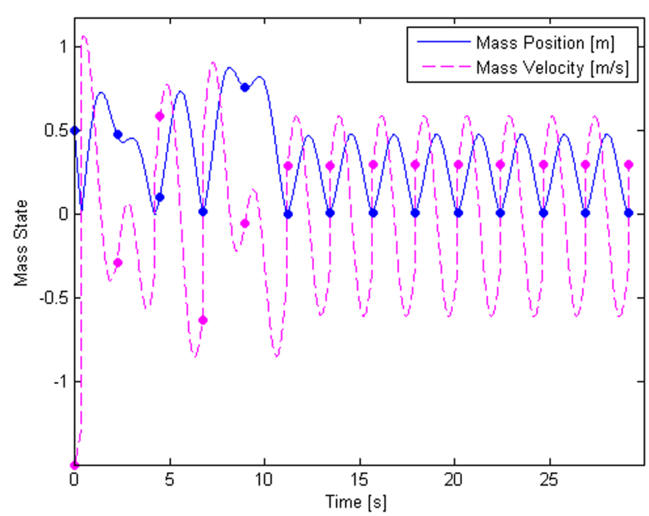

Fig. 6. Temporal evolution of the states (the position x and the velocity $\dot{x}$) of the mass.

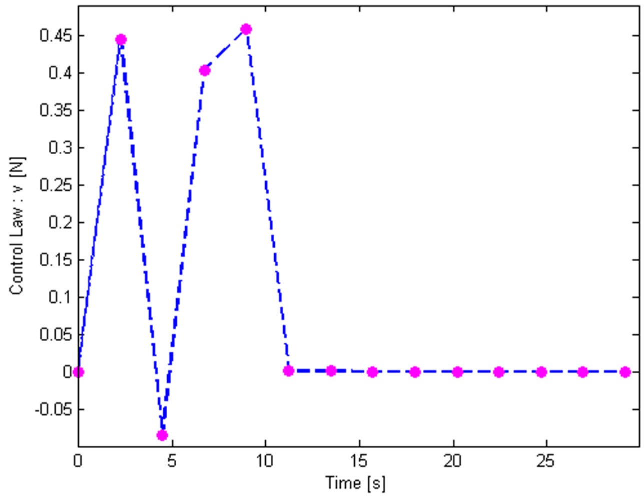

Fig. 7. Temporal evolution of the control law v.

map, we designed a state feedback controller to stabilize the unstable fixed point. We have demonstrated the effectiveness of our designed controller in the control of chaos in the impulsive hybrid linear non-autonomous dynamics of the impact oscillator.

REFERENCES

[1] M Lakshmanan and K Murali, *Chaos in nonlinear oscillators : Controlling and synchronization*, World Scientific, Singapore; 1996.

[2] A.L. Fradkov and A.Y. Pogromsky, *Introduction to Control of Oscillations and Chaos*, World Scientific, Singapore; 1996.

[3] M. Wiercigroch and B. De Kraker, *Applied nonlinear dynamics and chaos of mechanical systems with discontinuities*, World Scientific, Singapore; 2000.

[4] J. Awrejcewicz and C.-H. Lamarque, *Bifurcation And chaos In nonsmooth mechanical systems*, World Scientific, Singapore; 2003.

[5] B.H. Kaygisiz, I. Erkmen and A.M. Erkmen, Intelligent analysis of chaos roughness in regularity of walk for a two legged robot, *Chaos, Solitons and Fractals*, vol. 29(1), 2006, pp. 148–161.

[6] H. Gritli, S. Belghith and N. Khraeif, Intermittency and interior crisis as route to chaos in dynamic walking of two biped robots, *International Journal of Bifurcation and Chaos*, vol. 22(3), 2012, Paper No. 1250056, 19 p.

[7] H. Gritli, N. Khraeif and S. Belghith, Period-three route to chaos induced by a cyclic-fold bifurcation in passive dynamic walking of a compass-gait biped robot, *Communications in Nonlinear Science and Numerical Simulation*, vol. 17(11), 2012, pp 4356–4372.

[8] H. Gritli, S. Belghith and N. Khraeif, Cyclic-fold bifurcation and boundary crisis in dynamic walking of biped robots, *International Journal of Bifurcation and Chaos*, vol. 22(10), 2012, Paper No. 1250257, 15 p.

[9] H. Gritli, N. Khraeif and S. Belghith, Chaos control in passive walking dynamics of a compass-gait model, *Communications in Nonlinear Science and Numerical Simulation*, vol. 18(8), 2013, pp. 2048–2065.

[10] P. Thota and H. Dankowicz, Analysis of grazing bifurcations of quasiperiodic system attractors, *Physica D*, vol. 220, 2006, pp. 163–174.

[11] S. Lenci and G. Rega, Regular nonlinear dynamics and bifurcations of an impacting system under general periodic excitation, *Nonlinear Dynamics*, vol. 34, 2004, pp. 249–268.

[12] F. Pfeiffer and C. Glocker, *Multibody Dynamics with Unilateral Contacts*, Wiley-VCH Verlag, New York; 1996.

[13] D.Pun, S.L. Lua, S.S. Law and D.Q. Cao, Forced vibration of a multidegree impact oscillator, *Journal of Sound and Vibration*, vol. 213(3), 1998, pp. 447–466.

[14] D.J.Wagg, Periodic sticking motion in a two-degree-of-freedom impact oscillator, *International Journal of Non-Linear Mechanics*, vol. 40, 2005, pp. 1076–1087.

[15] C.J. Budd, *Non-Smooth Dynamical Systems and the Grazing Bifurcation*, In P.J. Aston, editor, Nonlinear Mathematics and its Applications, Cambridge University Press, 219–235; 1996.

[16] S.L.T. de Souza and I.L. Caldas, Calculation of Lyapunov exponents in systems with impacts, *Chaos, Solitons and Fractals*, vol. 19, 2004, pp. 569–579.

[17] S.L.T. de Souza and I.L. Caldas, Controlling chaotic orbits in mechanical systems with impacts, *Chaos, Solitons and Fractals*, vol. 19, 2004, pp. 171–178.

[18] P. Thota and H. Dankowicz, Continuous and discontinuous grazing bifurcations in impacting oscillators, *Physica D*, vol. 214, 2006, pp. 187–197.

[19] S.L.T. de Souza, I.L. Caldas and R.L. Viana, Damping control law for a chaotic impact oscillator, *Chaos, Solitons and Fractals* vol. 32, 2007, pp. 745–750.

[20] B.R. Andrievskii and A.L. Fradkov, Control of Chaos: Methods and Applications. I. Methods, *Automation and Remote Control*, vol. 64(5), 2003, pp. 673–713.

[21] B.R. Andrievskii and A.L. Fradkov, Control of Chaos: Methods and Applications. II. Applications, *Automation and Remote Control*, vol. 65(4), 2004, pp. 505–533.

[22] A.L. Fradkov and R.J. Evans, Control of chaos: Methods and applications in engineering, *Annual Reviews in Control*, vol. 29(1), 2005, pp. 33–56.

[23] A.L. Fradkov, R.J. Evans and B.R. Andrievsky, Control of chaos: methods and applications in mechanics, *Philosophical Transactions of The Royal Society A*, vol. 364(1846), 2006, pp. 2279–2307.

[24] E. Ott, C. Grebogi and J.A. Yorke, Controlling chaos, *Physical Review Letters*, vol. 64(11), 1990, pp. 1196–1199.

[25] T.S. Parker and L.O. Chua, *Practical numerical algorithms for chaotic systems*, Springer-Verlag, New York; 1989.

[26] P. Thotaa, X. Zhaob, and H. Dankowicz, Co-dimension-Two Grazing Bifurcations in Single-Degree-of-Freedom Impact Oscillators, *Journal of Computational and Nonlinear Dynamics*, vol. 1(4), 2006, pp. 328–335.